Available online at www.sciencedirect.com
SCIENCE DIRECT®
Thermochimica Acta 405 (2003) 255–268
thermochimica acta
www.elsevier.com/locate/tca

Melting of polymers by non-isothermal, temperature-modulated calorimetry: analysis of various irreversible latent heat contributions to the reversing heat capacity☆

M.L. Di Lorenzo[a,*], B. Wunderlich[b,c]

[a] *Istituto di Chimica e Tecnologia dei Polimeri (CNR), c/o Comprensorio Olivetti, Fabbr. 70, Via Campi Flegrei, 34-80078 Pozzuoli, NA, Italy*
[b] *Department of Chemistry, University of Tennessee, Knoxville, TN 37996-1600, USA*
[c] *Oak Ridge National Laboratory, Chemical and Analytical Sciences Division, Oak Ridge, TN 37831-6197, USA*

Received 31 May 2002; received in revised form 10 January 2003; accepted 1 April 2003

Abstract

This paper provides an analysis of contributions to the apparent, reversing heat capacity when measured by temperature-modulated differential scanning analysis (TMDSC) with an underlying heating rate in the temperature range where irreversible transitions with latent heats occur. To deconvolute the data of a TMDSC scan into a total and reversing part, it is common practice to use the sliding averages and the first harmonics of the Fourier series of temperature and heat-flow rate. Under certain conditions, this procedure produces erroneous reversing contributions which are detailed by experiment and simulation. Unless the response to the temperature modulation is linear, the total heat-flow rate is stationary, and the transition is truly reversible and occurs only once during the temperature scan, one cannot expect a true deconvolution of total and reversible effects. In the presence of multiple, irreversible transitions within a modulation period, however, each process involving latent heat can increase the modulation amplitude, as demonstrated by computer-simulation of polymer melting. As a result, the multiple transitions may give erroneously high latent heats when integrating the apparent reversing heat capacity with respect to temperature.

Keywords: Temperature-modulated calorimetry; Melting; Crystallization; Heat capacity; TMDSC

1. Introduction

Differential scanning calorimetry (DSC) measures the enthalpy (H) of a given sample by monitoring its changes with temperature (T) [the heat capacity, $C_p = (\partial H/\partial T)_{p,n}$], and during a transition [the latent heat, $L = (\partial \Delta H/\partial n)_{p,T}$]

$$\mathrm{d}H = \left(\frac{\partial H}{\partial T}\right)_{p,n} \mathrm{d}T + \left(\frac{\partial \Delta H}{\partial n}\right)_{p,T} \mathrm{d}n \qquad (1)$$

where p is the pressure and n the number of moles involved in the process. The variations in enthalpy are determined through the corresponding heat-flow rate, Φ. Only in case of no phase transition ($\mathrm{d}n = 0$) can the heat-flow rate be used to calculate thermodynamic data of heat capacity as $C_p = \Phi/q$ (where q is the linear heating rate in standard DSC). In all cases where $\mathrm{d}n \neq 0$, $C_p = \Phi/q$ is an "apparent" heat capacity

☆ The submitted manuscript has been authored by a contractor of the US Government under the contract number DOE-AC05-00OR22725. Accordingly, the US Government retains a non-exclusive, royalty-free license to publish or reproduce the published form of this contribution, or allow others to do so, for US Government purposes.

* Corresponding author.
E-mail address: diloren@mail.irtemp.na.cnr.it (M.L. Di Lorenzo).

0040-6031/$ – see front matter © 2003 Elsevier B.V. All rights reserved.
doi:10.1016/S0040-6031(03)00198-9

because it contains a latent heat contribution, and a separation of the baseline (or thermodynamic) heat capacity and latent heat effects must be undertaken by comparing the measured C_p values with thermodynamic data gained from measurements outside the transition region and extrapolation to the temperature in question considering the corresponding n [1].[1]

A more recent modification of DSC, temperature-modulated DSC or TMDSC, permits to superimpose a periodic variation to the standard, linear scan of the temperature and may allow to separate processes that are reversible during the temperature modulation [2]. The periodic variation of the temperature can be purely sinusoidal, which on linear response yields a heat-flow rate consisting of a phase-shifted, single cosine curve. Complex modulations, such as step or sawtooth changes of temperature contain multiple frequencies. In fact, the temperature variation of any periodic modulation of the sample temperature $T_s(t)$ can be described by a Fourier series:

$$T_s(t) = \langle T_s(t)\rangle + \sum_{\nu=1}^{\infty}[A_{T_{s,\nu}} \sin(\nu\omega t) + B_{T_{s,\nu}} \cos(\nu\omega t)] \quad (2)$$

where the underlying sample temperature, $\langle T_s(t)\rangle$, is the sliding average over the modulation period p ($p = 2\pi/\omega$, with ω representing the base frequency), while ν is an integer. The amplitudes $A_{T_{s,\nu}}$ and $B_{T_{s,\nu}}$ represent the νth Fourier harmonics. The heat-flow rate, Φ, can be represented by an analogous Fourier series. The reversing heat capacity is given by the ratio of the smoothed modulation amplitudes of the heat-flow rate, $A_{\Phi,\nu}$, and the temperature, $A_{T_{s,\nu}}$ [3]:

$$C_p(t) = \frac{\langle A_{\Phi,\nu}(t)\rangle}{\langle A_{T_{s,\nu}}(t)\rangle} \frac{K(\nu,\omega)}{\nu\omega} \quad (3)$$

where $K(\nu,\omega)$ is the frequency-dependent calibration constant. As long as the modulation starts at time $t = 0$ and is symmetric about $\langle q\rangle t$, the modulation is centro-symmetric and all $B_{T_{s,\nu}}$ are zero, i.e., their Fourier series contains only sinusoidal harmonics. A centro-symmetric sawtooth modulation simplifies the Fourier representation even further, as it shows only the odd harmonics ($\nu = 1, 3, 5$, etc.). The same holds for the heat-flow rate in case of linear response of the DSC to a sawtooth modulation of the sample temperature. Furthermore, representing the Fourier transform by the first harmonic only, limits the series of Eq. (2) to the single amplitude $A_{T_s} = A_{T_{s,1}}$. The error introduced by approximating a sawtooth modulation by the first harmonic only is of the order of 20–25%. It cancels when calculating the heat capacity with Eq. (3) because, with a linear response, the numerator and denominator of Eq. (3) have the same percentage changes in amplitude [4,5]. When, however, the measurements are not conducted under linear conditions, deconvolution of the modulated signal leads to errors in the evaluation of the heat capacity as will be shown below. Similarly, the sliding averages of $\langle T_s(t)\rangle$ and $\langle \Phi(t)\rangle$ must change linearly or be constant over the modulation cycle (stationarity condition) to be able to calculate a valid, apparent reversing C_p [6–8]. When true reversibility has not been established, the indicated heat-flow rates and heat capacity modulation are called "reversing" [2]. It will be shown in this paper, that much or even all of the "reversing heat capacity" may be irreversible.

Erroneous deconvolution of the modulated signal occurs frequently when transitions with high latent heats are analyzed in TMDSC with an underlying heating rate $\langle q\rangle$. If irreversible endotherms and exotherms overlap, as is often the case in the analysis of the melting of polymers, the reversing heat capacities may even give larger contributions than the total latent heat, as will be discussed in this paper. Excessive latent heats, however, are also observed in the analysis of the reversible melting. For example, the reversible melting range of indium is less than 0.10 K, but with a sufficiently high underlying heating rate, $\langle q\rangle$, and low modulation amplitude, melting is incomplete within the heating segment of the modulation cycle and recrystallization occurs in the following cooling segment as long as the temperature decreases below the melting temperature. The remaining crystals serve then as nuclei for this recrystallization. The next heating segment melts somewhat more of the indium and under appropriate conditions, several consecutive melting and crystallization peaks can be produced before melting is complete and recystallization cannot occur any more because of lack of nuclei. The sum of these transition peaks yields a latent heat which is much larger than

[1] For detail see: B. Wunderlich, Heat capacity of polymers, in: S.Z.D. Cheng (Ed.), Handbook of Thermal Analysis and Calorimetry, vol. 3, Elsevier, Amsterdam, 2002.

expected for a single melting and crystallization process, and the total melting peak is broadened [4,9].

The melting of macromolecules on heating in a DSC is generally represented in the apparent heat-capacity curve by a much broader endotherm than seen for small molecules. The melting is thought to be irreversible, although the measured temperatures can correspond under proper conditions to a "zero-entropy-production process". The zero-entropy-production melting may be either at the equilibrium temperature (in case the crystals are of equilibrium perfection) or at the temperature where a defect crystal transforms to a supercooled melt of identical thermodynamic stability [10]. The irreversible nature is seen when on reversing the temperature in the melting range there is no immediate regrowth of the just melted crystals until much lower temperatures have been reached (commonly at least 5–10 K, even in the presence of crystal nuclei). For such polymers it has been reported by non-isothermal TMDSC, that there is not only an apparent, reversing heat capacity in the melting range, but that its magnitude can even be higher than the total heat capacity [11–13]. The latter contains the sum of all reversible and irreversible contributions and can be easily determined from the sliding average over the modulation period [3]. It will be shown in this paper that such high reversing signals may be due to irreversible recrystallization and perfection after initial melting, followed by additional melting at higher temperature, rather than the multiple reversible melting described above for In [4,9].

The crystallization of polymers on cooling from the melt is irreversible and continues, in contrast to the melting, on reversing the temperature as long as the crystallization is incomplete. Such continuing irreversible, exothermic latent heat effect during cooling and heating can easily be separated from the heat-flow rate if the sliding average of one modulation period can be approximated by linear segments (stationarity [6–8]). For example, it was shown in the early publications on TMDSC that the cold crystallization in poly(ethylene terephthalate) shows no latent heat contribution in the reversing heat capacity [2]. The progress of crystallization can be gauged from the decrease in reversible, thermodynamic heat capacity as the crystallinity builds up [13]. All of the exothermic latent heat appears in the total, apparent heat capacity, together with the heat capacity effect, i.e., a full deconvolution of total and reversible effect is accomplished, the difference allowing a calculation of the irreversible effect. This well-understood example will not be further discussed in this paper.

More detailed analyses of the melting of polymers by quasi-isothermal TMDSC revealed, however, that in most polymers studied to date a very small portion of the sample melts truly reversibly [13]. This reversible melting occurs at the interface between crystal and melt, involving possibly the fold surfaces [12–18], the side surfaces [19–21], or both [13]. The fraction of sample that can melt and recrystallize reversibly has been quantified to be of the order of 0.03–0.3% of total crystallinity per temperature change of 1 K [12,14,19,22,23], but may be a much larger fraction of the crystal that melts at the same temperature range (specific, reversible crystallinity change) [24]. This creates the problem that the reversing latent heat to be derived from the apparent, reversing heat capacity measured by non-isothermal TMDSC may be attributed to irreversible as well as reversible effects. In this paper, several irreversible latent heat contributions are identified. Before quantitative analysis, these must be separated from the reversible effects. A common, but time-consuming method uses extended, quasi-isothermal experiments. In such quasi-isothermal TMDSC with an underlying heating rate $\langle q \rangle = 0$, one measures the reversing response over a long time span, so that all irreversible processes can decay and leave the reversible latent heat effect that can then be separated from the heat capacity.

2. Experimental

A poly(ether-co-amide) multiblock copolymer (PEBA) containing 80 wt.% of oligoimino(1-oxododecamethylene) and 20 wt.% of oligo(oxytetramethylene) was kindly supplied by ATOFINA Chemicals, Inc. The oligomer blocks are immiscible and form a microphase-separated structure in which both components can crystallize and melt. Measurements were performed with a Mettler DSC 820® heat-flux differential scanning calorimeter from Mettler-Toledo, Inc., equipped with a liquid-nitrogen cooling-accessory. Dry N_2 gas was purged through the DSC cell using a flow rate of 20 mL min^{-1}. The temperature of the

calorimeter was calibrated using the onsets of the transition peaks for indium (429.75 K), naphthalene (353.42 K), *n*-octane (116.4 K), acetone (177.9 K), cyclohexane (s/s 186.09 and s/l 297.7 K), cycloheptane (265.1 K), and tin (505.05 K) at a scanning rate of 10 K min^{-1}. The heat-flow rate was initially calibrated with the heat of fusion of indium (28.45 J g^{-1}), then refined with a baseline run of two empty aluminum pans, and a calibration run with sapphire as a standard [25].

Before analysis, the received sample chips were heated to 490 K, kept at this temperature for 10 min to erase any prior crystallization history, and then cooled with a rate of 10 K min^{-1} to 140 K. Standard DSC measurements were conducted at a heating rate of 10 K min^{-1}. The TMDSC was done with sawtooth modulation. The underlying heating rate, which is represented by the sliding average over one modulation cycle, was set to 2 K min^{-1}. One modulation period lasted 60 s. The heating segments had rates of 6 K min^{-1} for 30 s and were followed by cooling segments at rates of 2 K min^{-1} for 30 s. Subtraction of the underlying heating rate, $\langle q \rangle$, yields a pseudo-isothermal sawtooth with a rate of change of ± 4 K min^{-1}. A detailed calorimetric analysis of a series of PEBA has been presented earlier on this and other copolymer concentrations [26] and TMDSC data have also been published [12].

3. Results and discussion

3.1. Deconvolution of the experimental data

The total apparent specific heat capacity by standard DSC and the reversing apparent specific heat capacity by TMDSC of the 80/20 PEBA copolymer, measured over the temperature range where the oligoamide blocks melt are exhibited in Fig. 1 as the heavy and thin lines, respectively. The reversing C_p was calculated using the first harmonics of the heat-flow rate and temperature in Eq. (3). The thermodynamic heat capacity of the solid is given by the dotted line, that of the liquid, by the dashed line, both are calculated from the ATHAS Data Bank [1] (see Footnote 1). The detailed analyses of the thermal properties of PEBA copolymers as a function of composition and block length, as well as of reversibility of their melting process are not repeated here [12,26].

The major observations of the 80/20 PEBA copolymer is that the reversing contributions to the heat capacity shown in Fig. 1 increase beyond the total heat

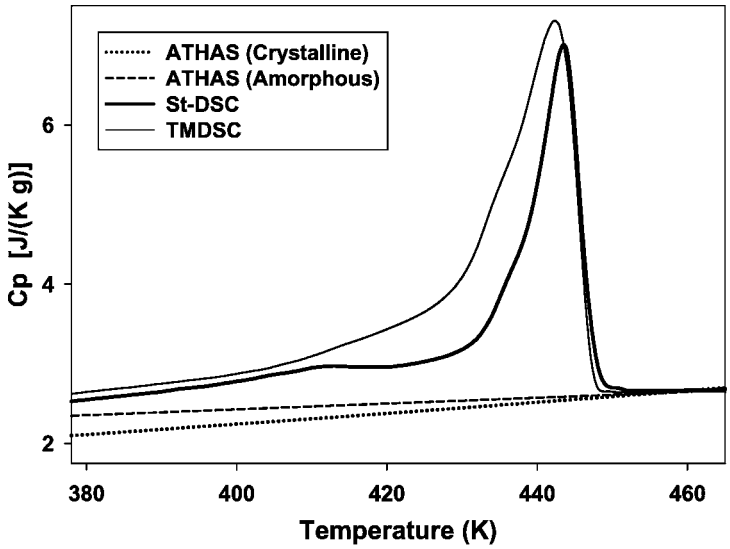

Fig. 1. Specific heat capacity of the 80/20 PEBA copolymer as a function of temperature. The thick line represents measurements by standard DSC, the thin line illustrates the reversing measurement by TMDSC with an underlying heating rate of 2 K min^{-1}. The dotted and dashed lines are the specific heat capacities of the solid and liquid, respectively, as calculated from the ATHAS data bank [1] (see Footnote 1).

capacity in the temperature region where the smaller and/or less perfect oligoamide crystals melt and then recrystallize to structures of higher thermodynamic stability. The integral over the baseline should result in the latent heat of the transition, but the reversing heat capacity yields a larger value than the total heat capacity, an unreasonable answer for a polymer that should melt largely irreversibly.

Above the melting region, the different harmonics of the Fourier series of the heat-flow rate and temperature are reported in Fig. 2a and b, respectively. In this temperature range the copolymer is liquid and

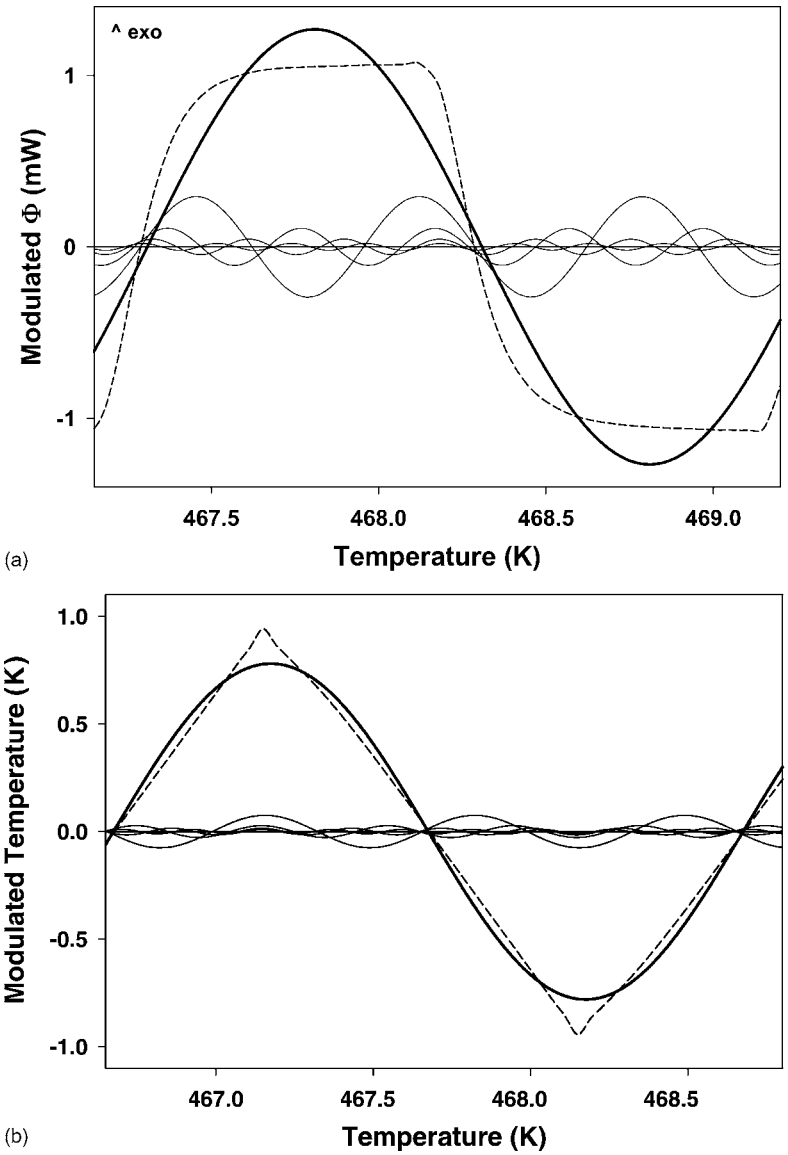

Fig. 2. (a) Modulated heat-flow rate and (b) temperature of the 80/20 PEBA copolymer measured above the melting temperature. Experimental data, deconvoluted to the pseudo-isothermal response, are represented by the dashed line. The thick line is the first harmonic, the thin lines are the higher (odd) harmonics of the Fourier series, up to the ninth. Even harmonics are negligible.

no transitions occur. One can see that there are no even-numbered harmonics, as expected for a sawtooth modulation when conditions of linearity and stationarity are fulfilled. Truncating the Fourier series after the first term produces only an approximation of the experimental data, but the overly large amplitude of the first harmonic is fully compensated by the higher terms of the series. It must be underlined that, for all harmonics shown in Fig. 2, the ratios of the amplitudes give the same heat capacity when inserted in Eq. (3) [4]. A non-linearity of $K(\nu, \omega)$ is expected at higher frequencies. Detailed methods for its empirical calibration have been worked out [27].

In the temperature range where melting occurs, an approximation of the experimental data with the first harmonic of the Fourier series is not possible, especially for the heat-flow-rate curve, as is displayed in Fig. 3a and b. The endotherms are larger than the exotherms, indicating a possible partial reversibility, but not full reversibility with multiple melting as discussed for In, above. Large distortions of both, the heat-flow rate and the temperature, cause the appearance of even terms of the Fourier series. In spite of these distortions, we used the first three odd terms of the Fourier series to calculate the reversing apparent heat capacity with Eq. (3), as done frequently. Obviously, for the even harmonics this is not possible since their temperature amplitudes are zero outside the transition region, as shown in Fig. 2b. The apparent heat capacities are displayed in Fig. 4. Very clearly, the apparent reversing heat capacity decreases rapidly with frequency [11,28]. In addition, one can observe sharp, small extraneous peaks at the melt-end of the third and fifth harmonic due to a rapid change in the stationarity, as was shown before whenever a sharp change in heat-flow rate occurs at the beginning and/or end of a transition [29]. Furthermore, there is an increase with frequency in errors outside the transition region. This limitation is based on the smaller temperature-amplitudes of the higher harmonics of a centro-symmetric sawtooth. They are inversely proportional to the square of the number of the harmonic [30].

The use of higher harmonics of the Fourier series to analyze the frequency-dependence of transitions, instead of performing several separate measurements at different modulation periods, has the advantage of subjecting the material under analysis to the same thermal history. It avoids the occurrence of different degrees of reorganization that could otherwise be induced by comparing separate runs with different modulation frequencies and complicates the analysis of the true frequency-dependence. It must be underlined, however, that the application of Eq. (3) requires linear response and stationarity [5–8]. The linear response of the heat-flow rate applies not only to the input of temperature modulation as altered by the sum of all distortions, but also to the thermal events governed by d*n* in Eq. (1), i.e., the change in n over a given temperature change must be reversible in the different time intervals. This is not the case in Fig. 4. When the temperature modulation is centro-symmetric, as programmed in the present experiment and seen outside the transition region illustrated in Fig. 2, the appearance of even harmonics in the heat-flow-rate response is an indication of a non-linear response, although its absence is not a proof of linearity. Unfortunately, during the main melting transition the temperature modulation itself does not follow the programmed true sawtooth and also has even harmonics, both due to calorimeter lags caused by the irreversible and reversing heats of transition.

The experiments have revealed three major points in the analysis of transitions with TMDSC in terms of reversing heat capacity. First, the values of the apparent, reversing heat capacity in Fig. 1 are much too large. Second, outside the transition region, reversible heat capacities can be measured in terms of the total, as well as the reversing heat-flow rate, as displayed in Figs. 1 and 2. Third, the frequency-dependence of the latent heat effect seems to indicate a decrease to the reversible level for high frequency, but does not approach the total heat capacity at low frequency as illustrated with Figs. 1–4. The following simulations are designed to understand the effect of overlapping, irreversible melting and crystallization and are mainly concerned with the magnitude of the reversing C_p. The frequency-dependence will be addressed in a later publication.

3.2. Simulation of the transitions

Melting of polymers is known to be largely irreversible [10], only a very small reversible contribution has been identified by quasi-isothermal TMDSC in the melting range for polymers of sufficiently high molar

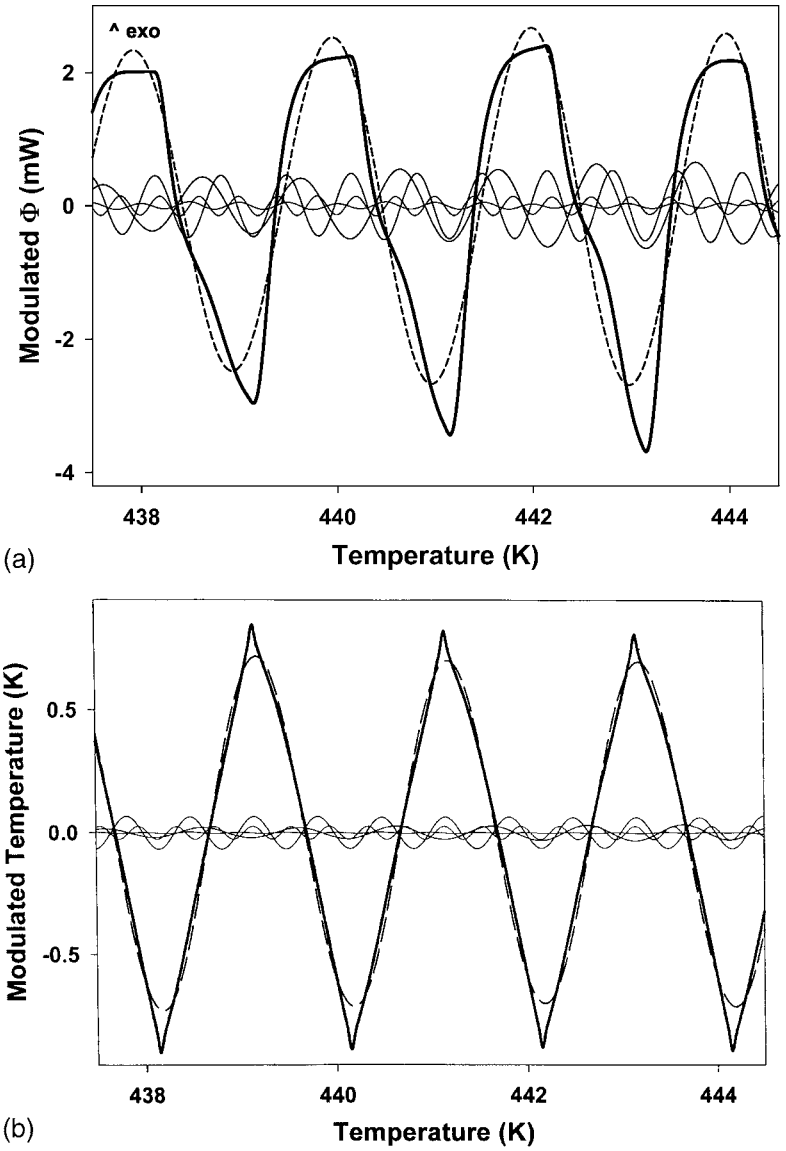

Fig. 3. (a) Modulated heat-flow rate and (b) temperature of the 80/20 PEBA copolymer measured during melting of the oligoamide blocks. The experimental data, deconvoluted to the pseudo-isothermal response, are represented by the heavy line, the dashed line is the first harmonic, the thin lines are the higher harmonics of the Fourier series, up to the fifth. Even as well as odd harmonics are present.

mass [13]. For the oligoamide blocks of the 80/20 PEBA copolymer used in this research, the amount of sample that melts truly reversibly at the maximum of the endothermic peak (440.2 K) over a temperature range of 1 K was quantified to be 0.3% of the total crystallinity [12]. This value was determined by quasi-isothermal analysis with a modulation amplitude of ± 0.5 K and a period of 60 s. The reversing heat capacity obtained with an underlying heating rate of 2 K min^{-1} is much larger, as shown in Figs. 1 and 4. The reasons for the overly large apparent reversing C_p are to be clarified next by the simulations.

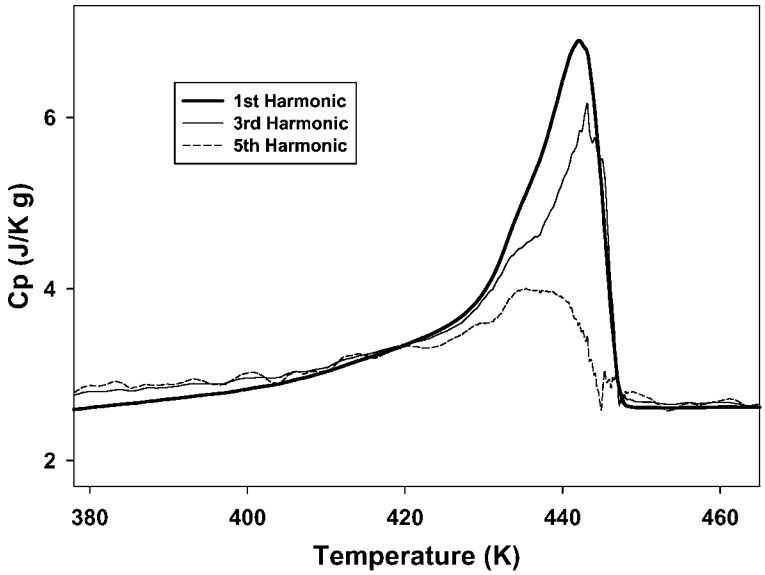

Fig. 4. Apparent reversing heat capacity of the 80/20 PEBA copolymer calculated using Eq. (3) for the first, third and fifth harmonics of the Fourier series.

In linear polymers, large amounts of reorganization take place during fusion of the crystallites, including partial or complete disordering of polymer chains, recrystallization, crystal thickening and perfection, all processes that involve evolution or absorption of latent heat [10]. Such processes occur also to a large extent in the poly(ether-amide) multiblock copolymers [12,26], and may contribute to the high apparent reversing C_p. Repeated fusions and recrystallizations with decreasing irreversibility may be induced by the temperature modulation coupled with an underlying change in temperature and increase the reversing latent heat. To substantiate this hypothesis, various modulated heat-flow rate curves were constructed to simulate fusion-recrystallization-annealing processes. The computer-designed modulated curves contain controlled amounts of reversible heat-flow rates and irreversible processes involving latent heat contributions. The aim is to correlate the apparent, reversing C_p obtained from deconvolution of the simulated curves to the different amounts of latent heats added to the modulated signal.

For the simulation of the transitions, different endotherms and exotherms of the amide blocks were added to experimental, fully reversible, modulated heat-flow rates which were measured at temperatures where no transitions occur, as illustrated in Fig. 2. Possible choices of irreversible melting and crystallization curves were taken from the upper and lower envelopes of the experimental modulated heat-flow rate of Fig. 5 after separation from the reversible heat capacity effect. Typical for polymers, the low-temperature parts of the endotherms are assumed to result from crystals that were grown at even lower temperature and may recrystallize at the melting temperature, but then only into crystals which melt at somewhat higher temperatures in overall irreversible processes. The recrystallized material gives rise to the so-called “annealing peaks” that are seen by DSC some 5–15 K above the crystallization temperature [10]. Even though parts of the endotherms and exotherms overlap and appear reversible by non-isothermal TMDSC, quasi-isothermal TMDSC would reveal their irreversibility.

The envelopes are chosen to keep the total heat capacity during the modulation at a level retaining approximate stationarity. Full linearity is guaranteed by the simulation condition which uses a constant $K(\nu, \omega)$. This also eliminates any frequency-dependence of the simulation data. Fusion and recrystallization were assumed to occur only during heating

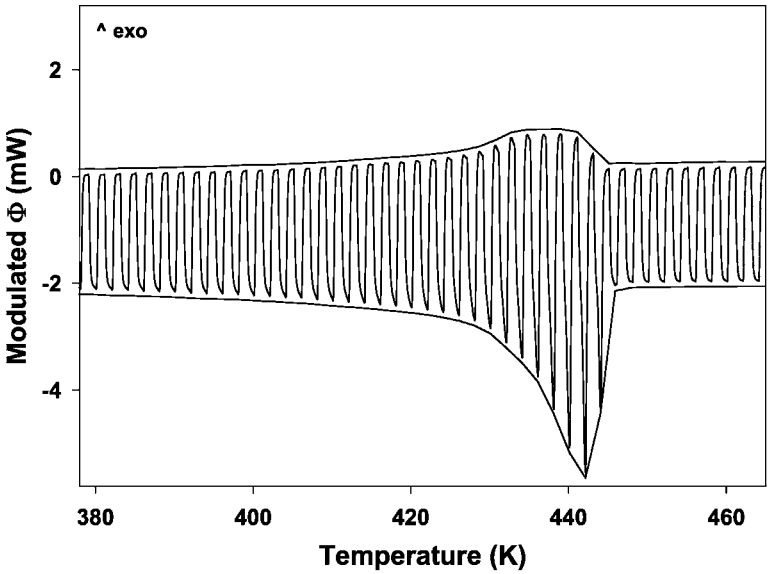

Fig. 5. Experimental, modulated heat-flow rate for the 80/20 PEBA copolymer. The upper and lower envelopes are shifted by 0.1 mW for clarity.

and cooling, respectively, the endotherm was added, thus, only to the heating portions of the sawtooth, and the exotherm to the cooling segments. This choice of addition of latent heat is observed on melting under zero-entropy-production conditions, but may not fully represent the crystallization during cooling, as was discussed for cold crystallization in Section 1. The simulated heat-flow-rate curves are shown in Fig. 6. They were obtained by accounting for melting peaks (endotherm M) and crystallization or annealing peaks (exotherm C). These simulations which model fusion of smaller and/or less perfect crystals and their annealing or recrystallization into structures of higher stability are ultimately to be compared to Fig. 1. In order to provide stationary conditions, the modulated heat-flow rate measured in a temperature region without transitions, as well as the envelopes of Fig. 5, were properly corrected to pseudo-isothermal.

To check the stationarity, the first four harmonics of the simulated heat-flow rate curves were determined in Fig. 7 for the data in Fig. 6a ("1M + 1C"). Outside the melting range the even harmonics are zero, suggesting stationarity [8]. Only at the end of the melting peak are the even harmonics non-zero for a few kelvins, but remain small relative to the odd harmonics, i.e., stationarity is approximated for most of the modulated data of Fig. 6a, as well as for all other modulated heat-flow rates of Fig. 6.

The reversing heat capacities for the simulated curves of Fig. 6 were calculated with Eq. (3), using the first harmonics of the modulated heat-flow rate and temperature. The results are presented in Fig. 8 and compared to the experimental TMDSC data of Fig. 1. For all simulations, a sizeable, reversing endothermic peak is observable. The addition of 0, 1, and 2 crystallization exotherms to a modulated heat-flow rate which contains a large irreversible endothermic transition produces an increase in the reversing C_p, as shown by comparison of the "1M + 0C", "1M + 1C" and "1M + 2C" plots. The extent of the increase depends on the amount of exotherm added to the modulated signal. A good representation of the experimental, reversing heat capacity represented by the heavy line can be obtained by arbitrarily shifting half of the exotherm by 6 K (Fig. 6d).

The first observation in Fig. 8 is that adding an irreversible latent heat to the heating cycle leads to a strong reversing signal under the given conditions ("1M + 0C," Fig. 6c). Even though only the heat capacity was chosen to be reversible, the irreversible

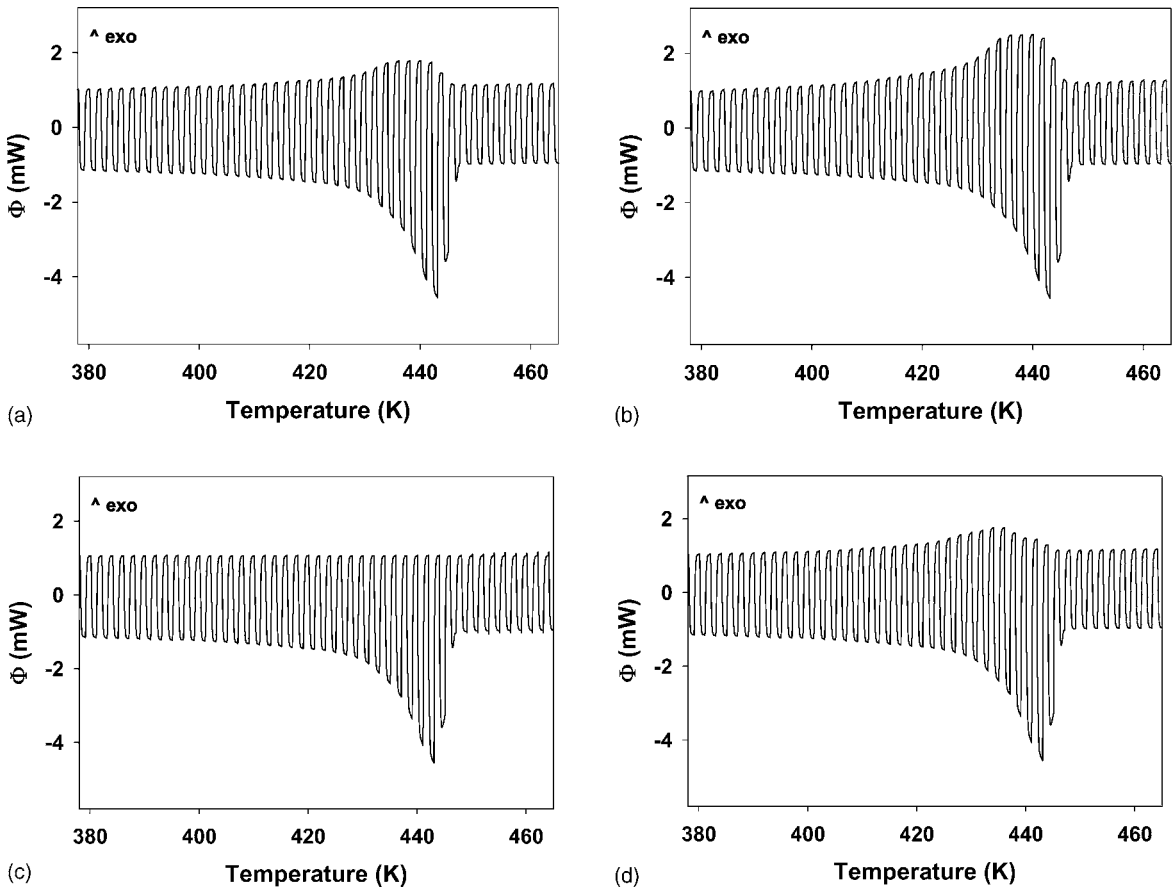

Fig. 6. Simulated heat-flow rates, obtained by adding latent heats to a reversible, modulated heat-flow rate, taken from an area without transitions and corrected to pseudo-isothermal conditions. (a) One melting and one crystallization curve ("1M + 1C", equivalent to Fig. 5); (b) one melting and two crystallization curves ("1M + 2C"); (c) one melting and no crystallization curve ("1M + 0C"); (d) one melting, 0.5 crystallization curve, and an additional 0.5 crystallization curve shifted by 6 K to lower temperature ("1M + 0.5C + 0.5A").

melting peak causes a large reversing peak. Its presence is caused by the erroneous deconvolution of the heat-flow rate $\Phi(t)$–$\langle\Phi(t)\rangle$ which, when expressed as a Fourier series, develops a large first harmonic, of which only the positive amplitude $A_{\Phi,1}$ enters into Eq. (3). The response $\Phi(t)$ to the modulated sample temperature is strongly non-linear.

Next, the addition of exothermic heat-flow rates at somewhat lower temperature causes even higher endothermic peaks in the reversing C_p that can easily exceed the total heat capacity and move the peak further to lower temperature, as is seen in Fig. 8. This is due to an increase of the amplitude of the heat-flow rate upon addition of any latent heat, as can also be deduced by comparing the modulated heat-flow rates of Fig. 6a–c (all plots of Fig. 6 are presented on the same scale). The reversing heat capacity of Eq. (3) depends, as before, on the magnitude of the heat-flow rate caused by the reversible heat capacity and the transitions, diminished by the sliding average $\langle\Phi(t)\rangle$ from $-p/2$ to $+p/2$, expressed as the proper fraction of the amplitude $A_{\Phi,1}$ of the first harmonic of the fitted Fourier series. In other words, it is the absolute value of each latent heat contribution in the separate heating and cooling cycles that determines the erroneous increase in the apparent reversing C_p, as both, endothermic and exothermic processes, are non-linear.

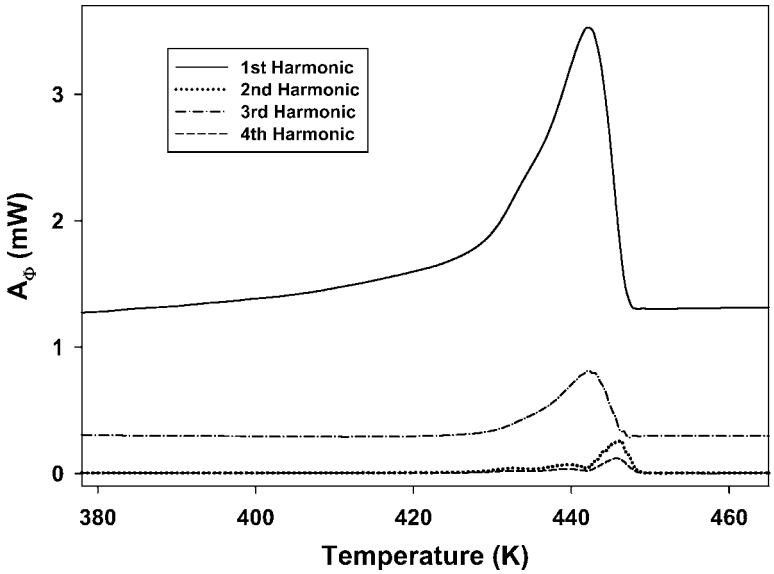

Fig. 7. Amplitudes of the first four harmonics of the modulated heat-flow rate of Fig. 6a ("1M + 1C" curve).

In order to clarify this point further, a modulated curve was constructed by adding one melting and subtracting one crystallization curve ("1M − 1C"), so that both M and C are endothermic. The resulting simulated heat-flow rate is displayed in Fig. 9a. As before with single endotherms, in this simulation both endotherms are added only to the heating portions of the modulated signal. The modulated heat-flow rate of

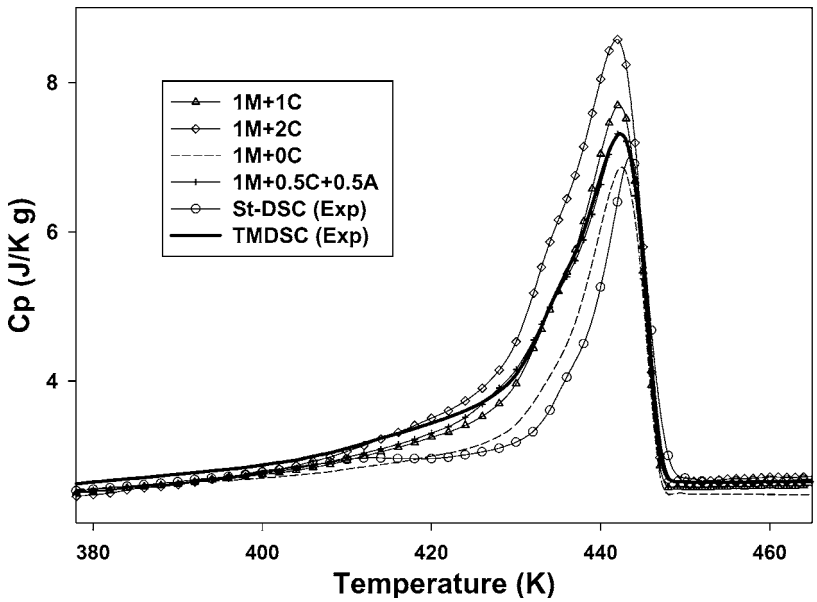

Fig. 8. Reversing apparent heat capacity calculated from the simulated raw data of Fig. 6, to be compared to the apparent heat capacity obtained from the experimental data reported in Fig. 1.

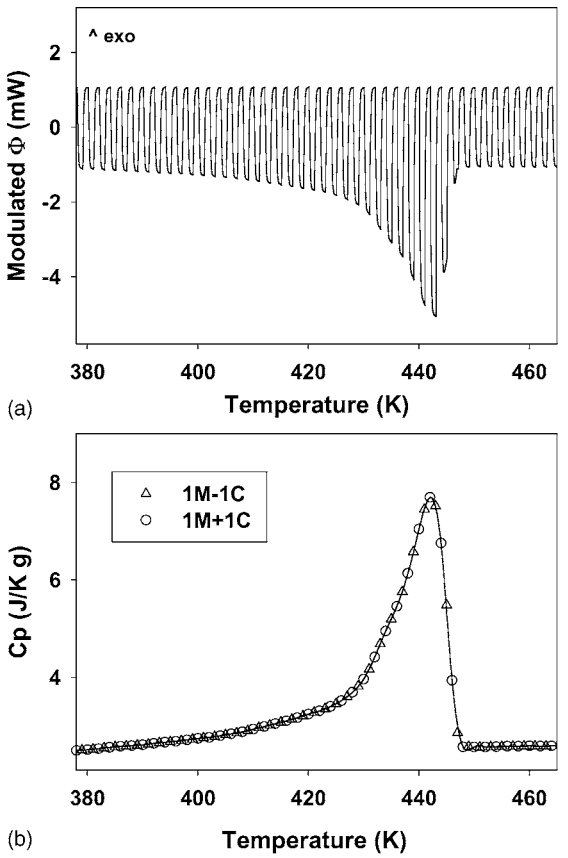

Fig. 9. (a) Simulated heat-flow rate obtained by adding one melting curve and subtracting one crystallization curve ("1M − 1C") to the same modulated heat-flow rate without transition used to build the curves of Fig. 6. (b) Reversing apparent heat capacity calculated from the heat-flux-rate data of (a) (curve ○). The reversing C_p obtained form the raw data of Fig. 6a, also reported in Fig. 8, is shown for comparison (curve Δ). The solid lines that connect the calculated reversing C_p points for the two curves overlap.

Fig. 9a is plotted to the same scale as in Fig. 6, so that the latent heat effects present in the simulated curves can be easily compared. The reversing C_p was calculated using the common deconvolution with the first harmonic of the Fourier series, and is shown in Fig. 9b. The plot of C_p vs. T of "1M − 1C" is identical to the "1M + 1C" case of Fig. 8, also redrawn in Fig. 9b.

These results show that measurements conducted by TMDSC with an underlying scanning rate do not permit proper separation of transitions that occur irreversibly and independently in the heating and cooling cycle. They appear as partially reversing and the reversing latent heat may exceed the total latent heat as is known from the analysis of the reversible melting of In. Neither the latent heat evolved nor absorbed in each process can be determined by a simple deconvolution of the experimental data. The mere analysis of the first harmonic (or of the higher harmonics) of the Fourier series leads to misleading interpretations of the reversing contributions. The matching of the experiment in Fig. 8 by the heat-flow rate of Fig. 6d, instead of the actually measured Fig. 6a indicates that the simulation is not following the experiment. Most likely the distortion of the temperature modulation, seen in Fig. 3b is at fault (compare to Fig. 2b). To analyze such complex processes, it is necessary to examine heat-flow-rate data in the time domain without an underlying heating rate (quasi-isothermally) and compare them to the modulated heat-flow rate measured in areas where no transitions occur [31,32]. After proper corrections are made to account for the variation of heat capacity with temperature, the latent heat evolved and absorbed in each cycle can be quantified. Analysis of the upper and lower envelopes of the modulated heat-flow rate, as reported in Fig. 5, can also permit to separate and quantify the latent heat evolved and absorbed by the sample, as will be shown in a forthcoming paper [33]. Only with these methods, may it become possible to study the various processes that occur on polymer melting. Coupling these analyses with quasi-isothermal measurements for extended times, that allow to extract truly reversible effects, it becomes possible to fully separate all the contributions that derive from the simultaneous effects of the underlying scanning rate and the temperature modulation, and from the continuous changes of the transition rates with temperature.

In general, the fraction of the sample that undergoes reversing melting depends on the experimental conditions chosen, being function of both the modulation amplitude and the frequency. Increasing the modulation amplitude or lowering the frequency, a higher apparent reversing heat capacity has been reported in all the studies conducted to date [11,13,34–40]. A decrease in the frequency of modulation permits a larger percentage of crystalline material to follow the modulation within a single temperature cycle. Similarly, an increase in modulation amplitude implies that a higher fraction of the crystallites is involved in the melting process that is added to the reversing signal.

According to the results of our simulation, if a higher fraction of the sample can follow the modulation, a larger amount of latent heat is absorbed or evolved per modulation segment, contributing to an increased apparent reversing heat capacity.

4. Conclusions

The investigation of polymer melting by TMDSC shows that the high apparent reversing C_p that is observed when using an underlying heating rate is attributed to errors in the deconvolution of the modulated data, linked to the approximations of the Fourier analysis. Three causes for the inclusion of excessive contributions in the reversing signal must be recognized when inspecting Fig. 8.

First, multiple reversible melting and crystallization are known to magnify the reversing melting peak, as shown first on the melting of In [4]. The same is true for partially irreversible recrystallization with remelting at higher temperature, as shown with the heat-flow rates of Fig. 6a–c. For quantitative analyses, these effects must be eliminated by long-time quasi-isothermal analysis to eliminate all irreversible and multiple processes.

Second, a large reversing contribution is already seen for the melting of polymers without reorganization or recrystallization, as simulated with Fig. 6c. Its large reversing effect arises from the special melting behavior of polymers. Polymers show a "zero-entropy-production melting" on heating, i.e., once melting starts on heating, it does not continue on cooling during the modulation. The crystallization, in contrast, may continue once it started on cooling after the modulation changes to the heating cycle. Finding the proper conditions of linearity and stationarity, crystallization can be properly deconvoluted from the reversible heat capacity, but melting cannot. The Fourier series of Fig. 3a matches during melting the endotherm with contributions in the heating and cooling segment to the first harmonic.

Third, an effort to match experiment and simulation in Fig. 8 leads to different heat-flow rates as seen in Figs. 5 and 6d. This result indicates that during the melting experiment, both the sample temperature and the heat-flow rate are distorted. The combination of the experimental heat-flow rate with the true sawtooth-modulated temperature with Eq. (3) shown in Fig. 8 ("1M + 1C") does not duplicate the experiment in Fig. 1.

This paper has extended the earlier simulation that dealt mainly with the loss of stationarity [29] and shown the pitfalls that arise from the special irreversibility that is typical for polymer crystallization and melting, i.e., that polymers melt close to their zero-entropy-production temperature, but crystallize mainly with a supercooling that is larger than can be explained by crystal nucleation. The additional reorganization, recrystallization, annealing, and remelting must naturally also be avoided for quantitative data. Most of the presently available data by non-isothermal TMDSC are qualitative, but as such can be understood in the frame of the present simulation. The separate problems that arise from changes of frequency and amplitude of modulation are to be addressed in the future.

Acknowledgements

The authors wish to thank Dr. Larry Judovits of ATOFINA Chemicals, Inc. (USA) for supplying the PEBA copolymer used in this research, as well as Dr. Maria Cristina Righetti of Istituto per i Processi Chimico-Fisici (CNR-Italy) and Dr. Pietro Di Lorenzo of Dipartimento di Matematica, Seconda Università di Napoli (Italy) for useful discussions. This work was supported by the Division of Materials Research, National Science Foundation, Polymers Program, Grant # DMR-9703692 and the Division of Materials Sciences and Engineering, Office of Basic Energy Sciences, US Department of Energy at Oak Ridge National Laboratory, managed and operated by UT-Battelle, LLC, for the US Department of Energy, under contract number DOE-AC05-00OR22725. Financial support from Italian National Research Council (Short-Term Mobility Program) is also acknowledged.

References

[1] Advanced Thermal Analysis System (ATHAS) Data Bank. http://web.utk.edu/~athas.
[2] M. Reading, Trends Polym. Sci. 1 (1993) 248.
[3] B. Wunderlich, Y. Jin, A. Boller, Thermochim. Acta 238 (1994) 277.

[4] B. Wunderlich, A. Boller, I. Okazaki, K. Ishikiriyama, W. Chen, J. Pak, I. Moon, R. Androsch, Thermochim. Acta 330 (1999) 21.
[5] R. Androsch, B. Wunderlich, Thermochim. Acta 333 (1999) 27.
[6] B. Wunderlich, J. Therm. Anal. 48 (1997) 207.
[7] M. Merzlyakov, C. Schick, Thermochim. Acta 330 (1999) 55.
[8] M. Merzlyakov, C. Schick, J. Therm. Anal. Calor. 61 (2001) 649.
[9] K. Ishikiriyama, A. Boller, B. Wunderlich, J. Therm. Anal. 50 (1997) 547.
[10] B. Wunderlich, Macromolecular Physics, vol. III, Crystal Melting, Academic Press, New York, 1980.
[11] M.C. Righetti, Thermochim. Acta 330 (1999) 131.
[12] M.L. Di Lorenzo, M. Pyda, B. Wunderlich, J. Polym. Sci. B 39 (2001) 2969.
[13] B. Wunderlich, Progr. Polym. Sci. 28 (2003) 383.
[14] B. Goderis, H. Reynaers, R. Scherrenberg, V.B.F. Mathot, M.H.J. Koch, Macromolecules 34 (2001) 1779.
[15] T. Albrecht, G.R. Strobl, Macromolecules 28 (1995) 5287.
[16] Y. Tanabe, G.R. Strobl, E.W. Fisher, Polymer 27 (1986) 1147.
[17] G.R. Strobl, M.J. Schneider, G. Voigt-Martin, J. Polym. Sci. B 18 (1980) 1361.
[18] J.M. Schultz, E.W. Fisher, O. Schaumburg, H.A. Zachmann, J. Polym. Sci. B 18 (1980) 239.
[19] R. Androsch, B. Wunderlich, Macromolecules 32 (1999) 7238.
[20] R. Androsch, B. Wunderlich, Macromolecules 33 (2000) 9076.
[21] R. Androsch, B. Wunderlich, Macromolecules 34 (2001) 2810.
[22] I. Okazaki, B. Wunderlich, Macromol. Chem., Rapid Commun. 18 (1997) 313.
[23] A. Wurm, M. Merzlyakow, C. Schick, J. Therm. Anal. Calor. 56 (1999) 1155.
[24] R. Androsch, B. Wunderlich, I. Kolesov, J. Polymer Sci. B, submitted for publication.
[25] D.G. Archer, J. Phys. Chem. Ref. Data 22 (1993) 1441.
[26] M.L. Di Lorenzo, M. Pyda, B. Wunderlich, J. Polym. Sci. B 39 (2001) 1594.
[27] R. Androsch, I. Moon, S. Kreitmeier, B. Wunderlich, Thermochim. Acta 357/358 (2000) 267.
[28] M. Merzlyakov, C. Schick, Thermochim. Acta 377 (2001) 193.
[29] M.L. Di Lorenzo, B. Wunderlich, J. Therm. Anal. Calor. 57 (1999) 459.
[30] B. Wunderlich, R. Androsch, M. Pyda, Y.K. Kwon, Thermochim. Acta 348 (2000) 181.
[31] K. Ishikiriyama, B. Wunderlich, Macromolecules 30 (1997) 4126.
[32] K. Ishikiriyama, B. Wunderlich, J. Polym. Sci. B 35 (1997) 1877.
[33] M. L. Di Lorenzo, M.C. Righetti, B. Wunderlich, in preparation.
[34] A. Toda, C. Tomita, M. Hikosaka, Y. Saruyama, Polymer 39 (1998) 5093.
[35] A.A. Minakov, C. Schick, Thermochim. Acta 330 (1999) 109.
[36] M. Merzlyakov, A. Wurm, M. Zorzut, C. Schick, J. Macromol. Sci. Phys. B 38 (1999) 1045.
[37] W. Hu, T. Albrecht, G. Strobl, Macromolecules 32 (1999) 7548.
[38] C. Schick, M. Merzlyakov, A.A. Minakov, A. Wurm, J. Therm. Anal. Calor. 59 (2000) 279.
[39] A. Toda, C. Tomita, M. Hikosaka, J. Mater. Sci. 35 (2000) 5085.
[40] R. Androsch, J. Polym. Sci. B 39 (2001) 750.